

Random Telegraph Signal and Flicker Noise In CMOS Image Sensor Using Column Source Follower Readout Circuits

Takahiro Kohara¹, Woonghee Lee¹, Koichi Mizobuchi² and Shigetoshi Sugawa¹

¹Graduate School of Engineering, Tohoku University, 6-6-11 Aza-Aoba, Aramaki, Aoba-ku, Sendai 980-8579, Japan

²DISP Development, Texas Instruments Japan, 2350 Kihara, Miho, Inashiki, Ibaraki 300-0496, Japan

Tel: +81-22-795-4833, Fax: +81-22-795-4834, E-mail: kohara@fff.niche.tohoku.ac.jp

1. Introduction

Recently, in CMOS image sensor the dark random noise of the pinned-photodiode 4T active-pixel design has decreased to around 2-e^- [1-5]. The approaches of introducing column amplifiers and column ADCs in CMOS image sensors have been reported in order to increase the SNR by relatively reducing the noises generated in the latter part of the column circuits. However, the noise reduction performances reach a limitation level due to the noises of pixels or column amplifiers themselves.

On the other hand, a low noise CMOS image sensor by using column amplifiers of the gains of about 1.0 with a column source follower (SF) has been reported [6]. In this sensor we have achieved readout circuits with below 1-e^- random noise, which naturally include not only on-chip column circuits but also off-chip circuits such as analog to digital converters. However, the degradation of the dark random noise caused by Random Telegraph Signal (RTS) in the pixel SF have been recognized as crucial issues in CMOS image sensor rather than charge coupled device [7-8].

In this paper, the random noise characteristics of CMOS image sensor have been analyzed using below 1-e^- noise readout circuits with column source follower architecture.

2. Device Structure

Fig. 1 shows the schematic diagram of the pixel and the column circuits including the peripheral block diagram of the image sensor. The sensor is as same as the previous work sensor [6].

3. Results and Discussion

Fig. 2 (a) and (b) shows the measured dark random noise histogram and the temporal output behavior of pixels belonging to each parts of the histogram. To examine dark random noise distribution of the sensor, the standard deviation of the consecutive 3200-frame outputs of each pixel at room temperature is defined as dark random noise. The histogram shows the asymmetric distribution of each pixel around the peak value, having a long tail toward high value of dark random noise. The temporal output behavior of pixel (A) and (B) is fairly constant. However, three discrete levels, where amplitude is about 1.5mV are found at pixel (C) and (D) because of RTS after correlated double sampling (CDS). In this sensor, this dark random noise with NOT Gaussian distribution is dominant source on random noise.

Fig. 3 shows the random noise with respect to each pixel location, which is consecutive pixel location at one row due to consider the non-uniformity of column readout circuits. In addition, we measure the four test patterns.

The first test is normal operation ('normal'). It is found that each pixel has the particular value of the dark random noise, which is always same value at some measurements. Therefore the dark random noise is due inherently to the individual pixel itself.

The second test is that the transfer transistor is always off (' $\phi T = \text{off}$ '). In this test the noise component of the charge transfer process are experimentally neglected. We have additionally carried out experiments of the temperature from 0°C to 60°C dependency of the dark random noise. We confirmed that the dark current was negligible at room temperature. Therefore comparing the random noise at 'normal' with that at ' $\phi T = \text{off}$ ', due to the charge transfer process the random noise increases. This charge transfer noise is about 2-e^- . But optimizing the charge transfer process in this sensor, the charge transfer noise can be fully minimized. Consequently this noise is not essentially critical problem in this sensor.

The third test is that floating diffusion (FD) is always tied to VR (' $\text{FD} = \text{VR}$ '). In this test FD is not floating, so that an effect of a feed back operation in the pixel SF is neglected. Comparing the random noise at ' $\phi T = \text{off}$ ' with that at ' $\text{FD} = \text{VR}$ ', it is found that the noise increases by about 1-e^- due to the feed back operation.

The last test is that the output of the pixel SF is always tied to V_{vclr} , which is a reset voltage of a vertical line (' $\text{out} = V_{\text{vclr}}$ '). In this case separating the pixels, we estimate the random noise of the readout circuits only. It is found that the random noise of the readout circuits including off-chip analog to digital converter is below 1-e^- . It shows that dominant source of the random noise is in the pixel rather than in the readout circuits.

Fig. 4 shows the dark random noise at 'normal' operation as a function of the high voltage level of ϕT . As the voltage applied to the transfer gate during the charge transfer process is lowered, the dark random noise reduces. Therefore the noise increases due to the pocket with inadequate charge transfer process. And charge trapping and de-trapping at the Si-SiO₂ interface during the charge transfer process may be also noise source [9].

Fig. 5 (a) shows the random noise at ' $\text{FD} = \text{VR}$ ' as a function of CDS period, which is a time from ' $\phi \text{NS} = \text{off}$ ' to ' $\phi \text{SS} = \text{off}$ '. It is found that the random noise decreases as the CDS period reduces from $100\mu\text{s}$ to about 0s . At 'normal' operation the CDS period is $4.56\mu\text{s}$ in this sensor because of the charge transfer process. Therefore the CDS architecture does not fully eliminate flicker noise and RTS. Consequently it is essential that an approach of reducing RTS and flicker noise themselves in the pixel SF, e.g., a buried-channel SF [10].

Fig. 5 (b) shows the measured power spectrum density (PSD) of each pixel. This is obtained by experimentally changing the CDS period at ' $\text{FD} = \text{VR}$ '. It is found that there are a $1/f$ spectrum (due to a flicker noise) and also a Lorentzian spectrum (due to a single trap RTS [11]).

Fig. 6 shows the random noise at ' $\text{FD} = \text{VR}$ ' as a function of VR. It is found that as VR is lowered, the random noise reduces because of the back-gate effect.

Fig. 7 shows the random noise at ' $\text{FD} = \text{VR}$ ' as a function of the pixel SF bias current (I_{bias}). It is found that the random noise decreases as the bias current increases.

4. Conclusion

The random noise characteristics of the CMOS image sensor with $1/4\text{-inch}$, SVGA, $4.5\text{-}\mu\text{m}$ pitch pixels fabricated by a $0.18\text{-}\mu\text{m}$ 2P3M technology have been analyzed using below 1-e^- noise readout circuits with a column source follower. As a result, it is found that dominant source of the dark random noise is RTS and flicker noise in the pixel SF. And in order to reduce the dark random noise in CMOS image sensor, RTS and flicker noise in the pixel SF must be reduced themselves.

References

- [1] Krymski et al., Proc. IEEE Workshop on CCDs and AISs, June 2003.
- [2] K. B. Cho et al., ISSCC Dig. Tech. Papers, pp.508-509, Feb. 2007.
- [3] H. Takahashi et al., ISSCC Dig. Tech. Papers, pp.510-511, Feb. 2007.
- [4] M. Iwane et al., Proc. Int. Image Sensor Workshop, pp.295-298, June 2007.
- [5] S. Matsuo et al., Symposium on VLSI Circuits, June 2008.
- [6] T. Kohara et al., Symposium on VLSI Circuits, June 2009, to be published.
- [7] J. W. Kim et al., Proc. IEEE Workshop on CCDs and AISs, June 2005.
- [8] X. Wang et al., IEDM Tech. Dig. pp.115-118, 2006.
- [9] B. Fowler et al., Proc. Int. Image Sensor Workshop, pp.51-54, June 2007.
- [10] X. Wang et al., ISSCC Dig. Tech. Papers, pp.62-63, Feb. 2008.
- [11] M. J. Kirton et al., Advances in Physics, 38, 4, pp. 367-468, 1989

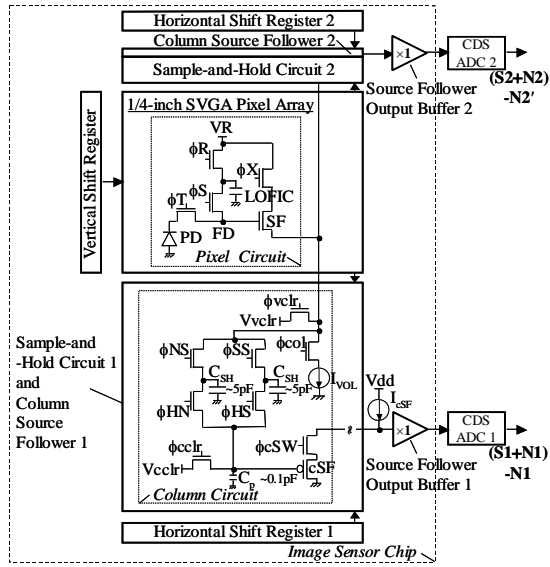


Fig.1 Block diagram with the schematic of pixel and column circuits.

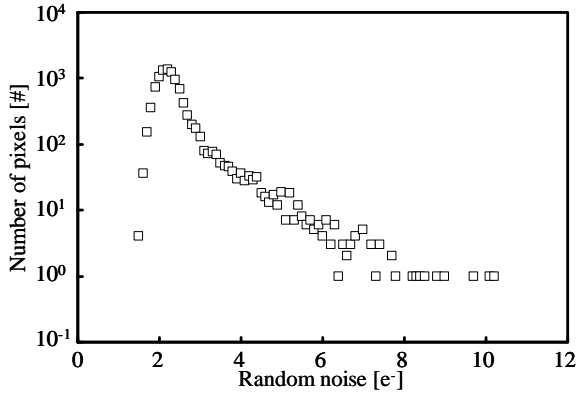


Fig.2 (a) Histogram of the dark random noise.

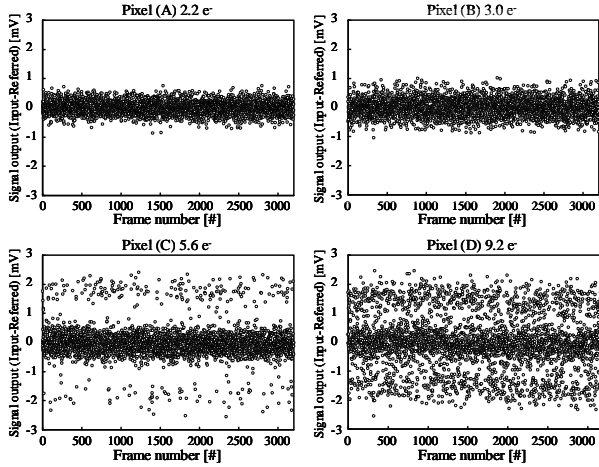


Fig. 2 (b) The temporal output behavior of each pixel.

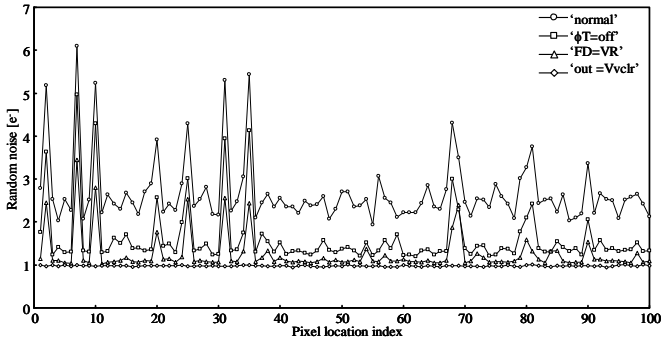


Fig.3 The random noise with respect to each pixel location (four test patterns).

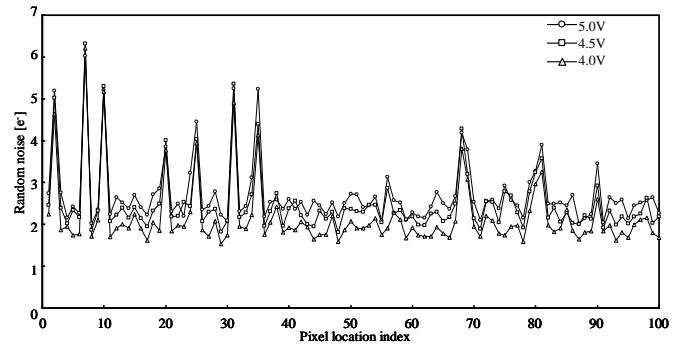


Fig.4 The random noise at 'normal' as a function of the high level of ϕT .

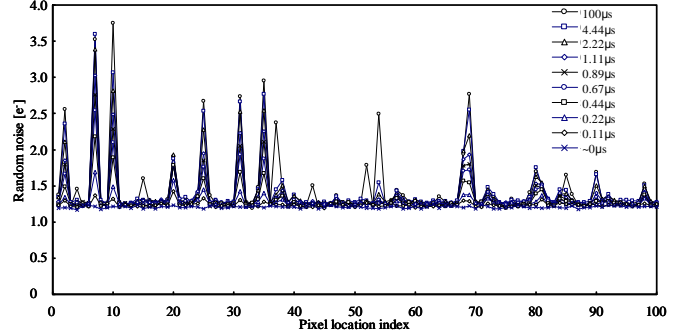


Fig.5 (a) The random noise at 'FD=VR' as a function of the CDS period.

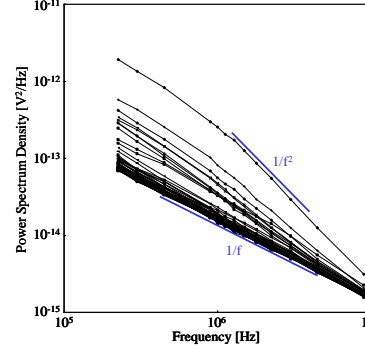


Fig.5 (b) Power spectrum density at 'FD=VR' of each pixel obtained by experimentally changing the CDS period.

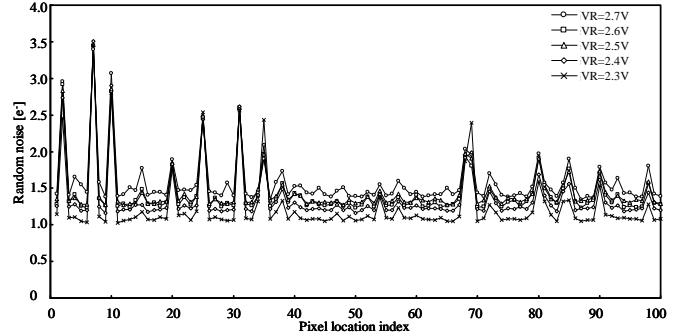


Fig.6 The random noise at 'FD=VR' as a function of VR.

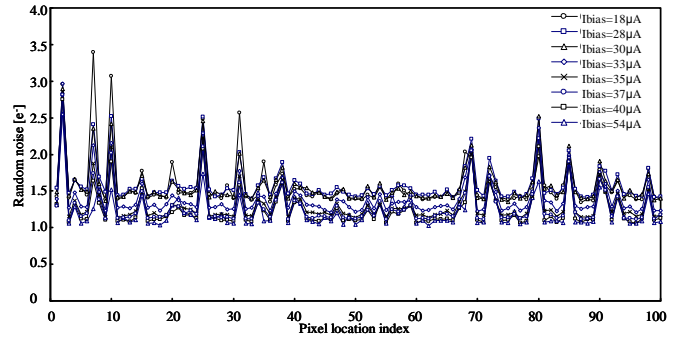


Fig.7 The random noise at 'FD=VR' as a function of the pixel SF bias current.